Facile and Rapid Synthesis of Durable SSZ-13 Catalyst Using Choline Chloride Template for Methanol-to-Olefins

xiongchao Lin
China University of Mining and Technology https://orcid.org/0000-0002-7096-2657
Sasha Yang (sashayang2009@gmail.com)
China University of Mining and Technology
Xiaojia Li
China University of Mining and Technology Beijing Campus
Caihong Wang
China University of Mining and Technology - Beijing Campus
Yonggang Wang
China University of Mining and Technology - Beijing Campus

Research

Keywords: SSZ-13, MTO, choline chloride template, catalyst

Posted Date: September 22nd, 2021

DOI: https://doi.org/10.21203/rs.3.rs-903025/v1

Abstract

In this study, a facile and rapid synthesis approach for SSZ-13 catalyst was proposed using choline chloride (CC) as template. The optimal synthesis condition was explored, and the catalytic performance for methanol-to-olefins (MTO) was examined. Results revealed that the appropriate ratio of soft template could meet the condition for rapid and ordered growth of catalyst crystals. Using environmentally friend and cheaper CC as template could greatly accelerate the formation of bi-hexagonal ring structure in SSZ-13 framework, and it could shorten the synthesis cycle to within 4 h. With a proper amount of CC addition (*i.e.*, $m(CC)/m(SiO_2)$ = 0.14), uniform and homogeneously distributed cubic SSZ-13 crystals were obtained with relatively lower aggregation. The catalyst synthesized with $m(CC)/m(SiO_2)$=0.14 demonstrated excellent porous features with a total specific surface area and mesopore volume of 641.706 $m^2.g^{-1}$ and 0.0377 $cm^3.g^{-1}$, respectively. The optimized strong and weak acid sites on the SSZ-13 were obtained by regulating the $m(CC)/m(SiO_2)$. As a typical acid catalytic reaction, the SSZ-13 catalyst with strong and weak acid sites exhibited bi-functional role. The lower amount of strong acid sites and larger amount of weak acid sites in the synthesized catalyst were conducive to the catalytic performance for MTO under relatively lower reaction temperature (450 ^oC). Consequently, the synthesized SSZ-13 showed a better conversion rate and lifetime than that of purchased one. The methanol conversion rate using synthesized catalyst was maintained over 95% within 120 min, and its lifetime was achieved to 172 min. The appropriate acidity and well-developed pore structure of synthesized SSZ-13 could slow down the carbon deposition rate and significantly increase the lifetime of the catalyst. Moreover, the initial selectivity of light olefin could maintain above 50% within 160 min. Eventually, the desirable features of synthesized SSZ-13 catalyst were thought be with good potential for industrial application.

1. Introduction

The methanol-to-olefins (MTO) reaction has been intensively studied in recent years with a particular focus on the development of high reactive and durable catalyst (Zhou 2016; Deimund 2016; Borodina 2015). Chabazite (CHA) zeolite with favorable structure is expected to be an ideal candidate for MTO (Tian 2015; Han 2017). As a promising CHA material, SSZ-13 with unique porous structure and high hydrothermal stability enables its high efficiency and selectivity (Ferri 2020; Liu 2017). The ordered crystal structure is quite essential for preparation of SSZ-13 zeolite. Conventionally, the very expensive N, N, N-trimethyl-1-adamantyl ammonium hydroxide (TMADaOH) was used as template for the synthesis of SSZ-13. Although the properties of the obtained hierarchical pore SSZ-13 are excellent, its synthesis process is complicated with inevitable environmental pollution caused by the toxic template precursor TMADaOH, and a long synthesis period (more than one week) was usually needed to compensate the slow growth of crystal. Therefore, the development of environmentally friendly and cost-effective template agent or non-template agent method with reduced synthesis cycle remains a challenge to be tackled. A novel route for rapid and facile synthesis of SSZ-13 catalyst is crucial and necessary.

The key factors influencing the synthesis of SSZ-13 zeolite are the template and processing conditions. The seed-guided method complying with core-shell growth mechanism in the crystallization process could affect the structure of molecular sieve. Synthesis of high purity SSZ-13 molecular sieve was achieved by crystallization at 100 ^{o}C for 4 days after exploring the influence of the amount of seeds (Jun 2016; Zeng 2020). Alternatively, the synthesis period of SSZ-13 zeolite was significantly reduced to several hours through steam-assisted crystallization without the aid of seed crystal (Wang 2015; Sommer 2010). Currently, an emerging process of template method for controlling mesoporous structure and adjusting the size of pore channel is now attracting more attentions. A series of growth-modifier assisted synthesis methods were established based on the disclosed particle attachment crystallization mechanism. Particularly, significant progress has been made in the use of polymers to control the synthesis of zeolite. Polymer hydrogels are three-dimensional networks of polymer chains that are cross-linked by physical means, which can be used as microreactors or nano-reactors to control the nucleation, assembly, and growth of zeolite (Li 2016; Zhu 2016). By combining TMADaOH and $C_{22-4-4}Br_2$ in the gelation process, hierarchical pore SSZ-13 molecular sieve was synthesized in one step (Zhang 2019). But such methods usually were with high synthesis cost and low yield, hindered its further industrial production.

Limited mass transfer in microporous molecular sieve and formation of coke in the cages could lead to a high deactivation propensity and low efficiency for catalytic MTO. By introducing hierarchical pore to the zeolite is one of the methods for the extensive utilization of CHA-type zeolite in MTO reaction (Xu 2015; Zhu 2014; Tang 2008). At present, extensive efforts have also been made to reduce the crystal size to nanoscale or introduce auxiliary mesopores/macropores to obtain the hierarchical pore materials (Wu 2014; Li 2019;). The use of organic guide agents, such as cationic polymer template agent, anionic polyacrylamide (APAM), and/or polydimethyldiallyl chloride (PDADMAC), to self-assemble could result in the formation of hierarchical pore with intermediate pore size of about 5 ~ 20 nm and micropore size of 0.8 nm (Janssen 2003; Xiao 2006). Such approaches have been proven to be a very useful practice to prepare mesoporous molecular sieves (Wardani 2019).

The status quo determines that the facile and rapid synthesis of SSZ-13 zeolite is crucial to a sustainable methanol economy. This study aimed to demonstrate a novel synthesis process for SSZ-13 zeolite based on traditional hydrothermal method. A series of process parameters were optimized, including the quaternary ammonium alkali, silica/alumina ratio, alkali/silicon ratio, water/silicon ratio, amount of seed, aging time, and crystallization temperature. Especially, the role of soft template choline chloride (CC) was revealed. In addition, the effects of CC on the porous characteristics and catalytic performance of SSZ-13 were also examined. It is expected to extent the synthesis of novel molecular sieve materials through a greener and more efficient process.

2. Experimental Section

2.1 Materials

Sodium hydroxide (NaOH), sodium meta-aluminate ($NaAlO_2$), aluminum isopropoxide ($C_9H_{21}AlO_3$), silica-sol LUDOX-40 ($mSiO_2{\cdot}nH_2O$), aluminum nitrate nonahydrate ($Al(NO_3)_3{\cdot}9H_2O$), ammonium chloride (NH_4Cl), choline chloride ($C_5H_{14}ClNO$) were purchased from Shanghai MackLin Biochemical Technology Co., LTD. The reagents used in this study were analytical reagent (AR).

2.2 Sample preparation

The catalysts were prepared using the hydrothermal synthesis method. In the synthesis process, the ratios of precursors were $n(SiO_2)/n(Al_2O_3) = 40$, $n(Na_2O)/n(SiO_2) = 0.4$, $n(H_2O)/n(SiO_2) = 12$. The ratio of $n(CC)/n(SiO_2)$ was varied from 0 to 0.32. The SSZ-13 crystal seed was added into the solution with a ratio of $n(seed)/n(SiO_2) = 0.4\%$. During the synthesis process, ca. 3.60 g NaOH and 0.49 g $NaAlO_2$ were dissolved in deionized water, followed by the addition of 2.30 g CC template agent. The solution was stirred for 10 min to ensure sufficient mixing. Subsequently, a commercially available SSZ-13 was introduced as homogenous seed. After intense stirring at room temperature for 20 min, 18.00 g inorganic silica sol (Ludox-40) was slowly added into the solution. Upon stirring for another 30 min, the initial gel was transferred to the hydrothermal reaction kettle lined with polytetrafluoroethylene, which was placed in a blast drying oven for constant temperature and static crystallization. After a period of crystallization, the products were washed to neutral and dried at 120 ^{o}C. Finally, the solid product was placed in a muffle furnace and calcined at 550 ^{o}C. The template agent was thus removed to obtain the Na-type SSZ-13 molecular sieve. NH_4-SSZ-13 molecular sieve was obtained by exchanging the Na-type SSZ-13 with 1 mol/L of NH_4Cl solution for 3 times, and sequentially the H-type SSZ-13 was prepared after drying and calcination.

2.3 Characterization of zeolites

X-ray diffraction (XRD) analysis was carried out on a Rigaku RINT ultimate-III powder diffractometer (Rigaku ltd. Co., Japan). The sample was in powder form. The 2θ range was 5 ~ 60° with a scanning rate of 10 °/min. Cu target K_β radiation was used with tube voltage of 40 kV and tube current of 30 mA. Scanning electron microscope (SEM, H-7650 Hitachi ltd. Co., Japan) was used to characterize the morphology and particle size of the materials prepared. FT-IR analyses of the raw and as-prepared materials were conducted using a FT/IR-615 JASCO (JASCO, ltd. Japan) spectrometer in transmission mode. For preparing pellets, the sample (ca. 1 mg) was further ground to powder with a size about 200 mesh and mixed with KBr (ca. 500 mg). Pellets of samples were prepared using the normal KBr procedure and were dried in an oven at 60°C for 12 h. All spectra were obtained at a resolution of 4 cm^{-1} in the range of 4000 ~ 400 cm^{-1} wave number. 32 scans per-spectrum were performed. Nitrogen absorption and desorption tests were performed using an Autosorb iQ Station 1 (Quantachrome, United States). Pore volume and size distribution were calculated with the DFT model. Before measurement, the samples were pretreated in vacuum at 200°C for 12 h. The surface acidity of as-prepared zeolite was determined by ammonia temperature-programmed desorption (NH_3-TPD). Chemical adsorption apparatus (BELCATII ltd. Co., Japan) equipped with thermal conductivity detector was used. About 0.05 g of molecular sieve was loaded into the U-type tube reactor, and then 0.04 g ultrafine silica wool was added in order to prevent the

gas from drifting away. The adsorbed gas was then removed from the sample by heating in an inert gas atmosphere to 350 ^{o}C. Subsequently, the sample was cooled to 100 ^{o}C under an ammonia flow (flow rate 30 sccm, time 60 min) to achieve saturated adsorption. The He (30 mL/min) was injected for about 30 min to remove the physically adsorbed ammonia gas. Finally, TPD was heated to 700 ^{o}C in He atmosphere at a heating rate of 10 ^{o}C/min, and the amount of ammonia gas de-adsorbed from the acidic center was measured by thermal conductivity cell detector.

2.4 Evaluation of the catalytic performance

The MTO reaction was conducted on a fixed-bed quartz tube reactor (φ6 mm) using the as-prepared catalysts. The schematic of the fixed-bed reactor is illustrated in Fig. 1. About 300 mg molecular sieve catalyst (40 ~ 60 mesh) and 2.7 g quartz sand were well mixed and loaded into the reactor. The reactor was then heated to 550 ^{o}C at an interval of 10 ^{o}C/min to firstly remove the impurities adsorbed in molecular sieve for 1 h. And subsequently, the temperature was set to reaction temperature of 450 ^{o}C for 20 min. The weight hourly space velocity (WHSV) was 3 h^{-1}. The reaction products were identified and quantified through in-situ gas chromatograph (GC).

3. Results And Discussion

3.1 The crystal structure of synthesized SSZ-13

Primarily, a series of processing parameters, including the silica/alumina ratio, alkali/silicon ratio, water/silicon ratio, amount of seed, aging time, and crystallization temperature, were systematically optimized (as shown in supporting information Fig. S1). The key factor, namely the ratio of n(CC)/n(SiO_2), impacting the catalyst feature was principally focused. The XRD patterns of synthesized materials with different ratio of m(CC)/m(SiO_2) were presented in Fig. 2. Without the addition of CC template, the product was ANA-zeolite in pure phase (Fig. 2a). With the addition of CC template agent, the characteristic peak of ANA at 2θ = 15.9° gradually disappeared. The secondary structural unit of SSZ-13 was gradually formed in the mixed gel. As the m(CC)/m(SiO_2) = 0.14, pure SSZ-13 phase generated with a relative crystallinity of 101.2% (Fig. 2d, Table S1). It could obviously prove that the CC template greatly accelerated the formation of SSZ-13 structure. In addition, the excessively increasing the amount of CC template agent did not show apparent influence on the crystal structure of SSZ-13. Therefore, the m(CC)/m(SiO_2) ratio of 0.14 was the optimal condition to obtain a fully crystallized SSZ-13 molecular sieve with low cost (taking the commercially available SSZ-13 as a reference). The optimized condition details for the synthesis of SSZ-13 using CC template were described in supporting information and **Fig.S1**.

3.2 Morphology of catalysts

Figure 3 shows the SEM images of prepared SSZ-13 catalysts with different ratios of the m(CC)/m(SiO_2) = 0.07, 0.14 and 0.32, respectively. The sample prepared by m(CC)/m(SiO_2) = 0.07 was irregular particles

dominated by cubic shape and mixed with many different size crystals (Fig. 3a). It was thought that with lower addition of template agent, it was hard to achieve completely crystallization of amorphous gel into regular SSZ-13 molecular sieves. The particles were severely aggregated rather than homogeneously dispersive. The serious aggregation was ascribed to the lack of specification template agent and slow nucleation rate, as well as the insufficient crystal nucleus formation during the hydrothermal synthesis. With the m(CC)/m(SiO_2) ratio increased to 0.14, the irregular particles gradually disappeared, as shown in Fig. 3b. Even though the particles demonstrated slightly aggregation, the cubic crystals were relatively homogeneously distributed. The appropriate amount of template could meet the condition for rapid and ordered growth of catalyst crystals. Compared with synthesized sample with m(CC)/m(SiO_2) = 0.14, it could be clearly seen that the purchased commercial SSZ-13 sample was still in serious agglomeration form (Fig. 3d). It may indicate more excellent performance of as-prepared SSZ-13 using choline chloride template. With the m(CC)/m(SiO_2) ratio increased to 0.32, the particles became more terrible agglomeration (Fig. 3c), and the crystal morphology changed to be ambiguous. It was considered that the excessive amount of choline chloride template might promote the growth of larger size crystal, and consequently induce the locally sudden agglomeration. It was consistency with the XRD analysis that the m(CC)/m(SiO_2) = 01.4 was the optimal condition to obtain relative uniform and cubic particles without undesired agglomeration. And besides, the synthesis time was shortened to within 4 h, highly improved the preparing efficiency.

3.3 Variation of microstructure

The FTIR spectra of the SSZ-13 prepared with different m(CC)/m(SiO_2) ratios are shown in Fig. 4. Roughly, the peak vibrations of the synthesized samples were similar. The typical absorption peaks at 460, 526, 647, 777 and 1069 cm^{-1} were assigned to the SSZ-13 molecular sieve. The asymmetric stretching of Si-O-Si or Al-O-Si bond was a wide and strong peak near 1069 cm^{-1}, which was classified to be T-O-T vibration. Likewise, the peak at 777 cm^{-1} was the symmetrical vibration of Al-O. The peak vibration of a single six-member ring was at around 526 cm^{-1}. And at ca. 647 cm^{-1} was the peak vibration of double six-member ring. The strong absorption peak near 460 cm^{-1} was attributed to the bending vibration of Si-O in silicon-oxygen tetrahedron. The peaks at 1631, 3450 and 3615 cm^{-1} were the stretching of -OH. Two weak peaks at 2924 and 2849 cm^{-1} were ascribed to the stretching of -CH_2- derived from the residual organic template.

From Fig. 4, it can be clearly seen that the absorption peak at 1069 cm^{-1} became narrower with the m(CC)/m(SiO_2) ratio increase, indicating the gradually ordered and regular of the SSZ-13 crystal. The FTIR is extremely sensitive to the change of silica-alumina microstructure. With the addition of chorine chloride, absorption peaks at 647 and 526 cm^{-1} gradually appeared revealing the formation of bi-hexagonal ring unit in SSZ-13 framework. The formation of bi-hexagonal ring structure proved the template facilitating the crystallization process; likely, the increase of the absorption peak intensity suggested the crystallization getting gradually completed. Obviously, the catalyst prepared with

$m(CC)/m(SiO_2)$ = 0.14 showed the sharpest peak at 1069 cm^{-1} (Fig. 4c) implying the relative ordered Si-O-Si or Al-O-Si structure without extra distortion. It is consistent with the results discussed in XRD and SEM analyses.

3.4 the pore structure of as-prepared SSZ-13

The reactions on molecular sieve are very sensitive to the framework structure. The adsorption-desorption isotherms of synthesized samples with different $m(CC)/m(SiO_2)$ are shown in Fig. 5. And their surface area and pore volume are listed in Table 1. The results suggested that the synthesized SSZ-13 samples possessed Langmuir adsorption-desorption isothermal curves. The SSZ-13 samples had homogenously distributed microporous channels. In the low-pressure region ($10^{-6} < P/P_0 < 0.01$), an obvious spike was observed, which was induced by the adsorption of nitrogen molecules in the micropores. The adsorption plateau appeared at $P/P_0 > 0.1$, approaching to adsorption saturation. At $P/P_0 > 0.95$, the adsorption isotherm gradually increased and arrived the highest point due to capillary condensation. At the relative pressure P/P_0 = 0.45, desorption curve is closed to form the hysteretic ring, indicating the synthesized zeolite contained stacking mesopores formed by the accumulation of small crystal particles. Such small particles could be also found in the SEM images (Fig. 3). Particularly, the catalyst prepared with $m(CC)/m(SiO_2)$ = 0.14 showed more significant mesopore structure with an obvious hysteretic ring (Fig. 5b). As can be seen from Table 1, the total specific surface area of samples prepared at $m(CC)/m(SiO_2)$ = 0.07, 0.14 and 0.32 were 419.177 $m^2.g^{-1}$, 641.706 $m^2.g^{-1}$, and 583.623 $m^2.g^{-1}$, respectively; and the mesopore volume were 0.0162, 0.0377, and 0.0250 $cm^3.g^{-1}$, respectively. Undoubtedly, the proper amount of template agent with $m(CC)/m(SiO_2)$ = 0.14 achieved the largest specific surface area and highest meso-pore volume.

Table 1
Pore structure characteristics of as-prepared zeolites

Sample	$S_{BET}(m^2.g^{-1})$	$S_{mic}(m^2.g^{-1})$	$S_{ext}(m^2.g^{-1})$	$V_{mic}(cm^3.g^{-1})$	$V_{meso}(cm^3.g^{-1})$
$m(CC)/m(SiO_2)$ = 0.07	419.177	410.642	8.535	0.15699	0.0162
$m(CC)/m(SiO_2)$ = 0.14	641.706	636.058	5.648	0.23980	0.0377
$m(CC)/m(SiO_2)$ = 0.32	583.623	569.036	14.586	0.20884	0.0250

3.5 the acidity of the SSZ-13

The ammonia temperature-programmed desorption method (NH_3-TPD) could reveal the acid properties of the as-prepared SSZ-13. The NH_3-TPD of the SSZ-13 catalysts prepared with different $m(CC)/m(SiO_2)$ and purchased SSZ-13 were presented in Fig. 6. There were two typical desorption peaks found in the

samples. The peak near 200 ^{o}C was the low temperature desorption region, which was attributed to the interaction between acid level and ammonia gas. NH_3 could be desorbed from these weakly acidic surface hydroxyl groups, forming the weak acid potential of SSZ-13. The peak in the range of 490 ~ 540 ^{o}C was the high temperature desorption peak from the bridging hydroxyl group (≡ Si-OH-Al≡), corresponding to the strong acid center. The desorption peaks in the low temperature region were stronger, suggesting the weak acid sites were dominant. With the increase of m(CC)/m(SiO_2), the strong acid potential tended to shift to high temperature region. The corresponding peak area increased greatly at m(CC)/m(SiO_2) = 0.14. From Table 2, the weak and strong acidity of m(CC)/m(SiO_2) = 0.14 were 0.672 and 0.553 mmol/g, respectively. In accordance with the SEM images, at m(CC)/m(SiO_2) = 0.14, the particle size distribution became more uniform and the specific surface area increased significantly, indicating a larger amount of acid sites on the surface. The optimized strong and weak acid sites was obtained by regulated the m(CC)/m(SiO_2), which would be conducive to the catalytic performance of such catalyst under relatively low temperatures.

Table 2
Acidity of as-prepared SSZ-13 measured by NH_3-TPD

Samples	Weak acid site		Strong acid site	
	Temperature (°C)	Acidity (mmol/g)	Temperature (°C)	Acidity (mmol/g)
m(CC)/m(SiO_2) = 0.07	200	0.424	505	0.507
m(CC)/m(SiO_2) = 0.14	210	0.672	536	0.553
m(CC)/m(SiO_2) = 0.32	201	0.450	511	0.801
SSZ-13	203	0.354	510	0.558

3.6 Catalytic performance for MTO

Based on the optimal conditions described, the catalytic activity of the synthesized SSZ-13 material for MTO reaction was evaluated. As a typical acid catalytic reaction, the SSZ-13 would demonstrate the role of bi-functional catalyst. The catalytic performance of purchased (using the TMAdaOH as template) and synthesized (using the CC as template) SSZ-13 for MTO was shown in Figs. 7 and 8. The products were mainly C1 ~ C3 alkanes and alkenes. The ethylene and propylene were the dominant compounds, and their yield reached the highest at 60 ~ 90 min. The yields were maintained over 35% during the test. The main by-products were CH_4, C_2H_6, and C_3H_8. In the early stage (before 40 min) of the MTO reaction, the methanol was firstly decarbonylated for the formation of intermediates, such as acetate, formate, methyl acetate, and dimethoxymethane; while the zeolite was carbonylated during the induction period. The yield of by-products was continuously decreased during the reaction period indicating the improvement of reaction selectivity and deactivation of catalyst.

Both the SSZ-13 catalysts maintained a high methanol conversion rate over 95% within a reaction time of 120 min, and it would drastically drop down to ca. 80% in 80 min. Eventually, the conversion rate would maintain at ca 75% in a long reaction period (Fig. 7). The synthesized SSZ-13 showed a better conversion rate than that of purchased one. The catalytic lifetime of the molecular sieve was defined as duration that the methanol conversion was kept above 90%, *i.e.* the time from the beginning of the reaction to the methanol conversion dropping to 90%. From the NH_3-TPD analyses, the weak acidity of synthesized and purchased SSZ-13 were 0.354 and 0.450 mmol/g, respectively; and the strong acidity were 0.558 and 0.721 mmol/g, respectively. Consequently, the as-prepared and purchased samples exhibited obvious differences in the catalytic lifetime. Their catalyst lifetimes were 172 and 160 min, respectively. The reaction intermediates, such as methyl benzene, would be gradually converted into polycyclic aromatic hydrocarbons, which thus might accumulate on the internal surface and outside the cage of SSZ-13, leading to congestion of channel and lower the mass transfer rate. Eventually, it would become difficult for the reactants to contact with the active center resulting in catalyst deactivation. It was considered that the appropriate acidity and well-developed pore structure of synthesized SSZ-13 could slow down the carbon deposition rate and significantly increase the lifetime of the catalyst. Primarily, the formation of dimethyl ether initiated on the weak acid center, and sequentially the conversion of dimethyl ether to light olefins would occur on the strong acid center (Cheng 2016).

Both the two SSZ-13 catalysts showed induction period where the selectivity was quite low in the beginning 40 min, as shown in Fig. 8. The light olefin selectivity reached the highest at the reaction time of ca. 60 min. The methanol adsorbed at the acid site was the first step of MTO conversion; and the deprotonation of carbenium ions and shift of methyl groups would be the followed reaction. The framework structure of SSZ-13 could accelerate the deprotonation of carbenium ions and convert the methyl group into the alkene (Li 2020). Such induction reaction could be occurred under low reaction temperature (i.e., < 450 ^{o}C). The active hydrocarbon species would form inside the zeolite at the initial stage. Theoretically, the synthesized SSZ-13 with higher acidity would possess strong adsorption capacity. The light olefine selectivity of as-prepared SSZ-13 was slightly lower than that of purchased SSZ-13. It was thus thought that the excessive micropore hindered the timely desorption and diffusion of intermediate products, and consequently reduced the light olefin selectivity. Although the light olefin selectivity of synthesized SSZ-13 was slightly lower than that of purchased SSZ-13, the initial selectivity could maintain above 50% within 160 min with the conversion rate over 90%. The larger amount of weak acid sites and relative smaller amount of strong acid sites on the as-prepared SSZ-13 using choline chloride as template were beneficial for the low temperature catalytic performance and longer lifetime.

4. Conclusions

The time-consuming, expensive, and polluting synthesis process are the key drawbacks for the industrial utilization of SSZ-13 catalyst in MTO technology. This work demonstrated a facile and rapid synthesis approach for SSZ-13 using choline chloride as template. The optimal synthesis condition was explored, and the catalytic performance for methanol-to-olefins (MTO) was examined. The choline chloride was

proved to be effective for the synthesis of SSZ-13. An appropriate ratio of soft template could meet the condition for rapid and ordered growth of catalyst crystals. The special molecular structure of choline chloride could greatly accelerate the formation of bi-hexagonal ring structure in SSZ-13 framework, and it could shorten the synthesis cycle to within 4 h. With a proper amount of choline chloride addition (*i.e.*, $m(CC)/m(SiO_2) = 0.14$), uniform and homogeneously distributed cubic SSZ-13 crystals were obtained with relatively lower aggregation. The catalyst synthesized with $m(CC)/m(SiO_2) = 0.14$ demonstrated excellent porous features with a total specific surface area and mesopore volume of 641.706 $m^2.g^{-1}$ and 0.0377 $cm^3.g^{-1}$, respectively. The optimized strong and weak acid sites on the SSZ-13 were obtained by regulating the $m(CC)/m(SiO_2)$. As a typical acid catalytic reaction, the SSZ-13 catalyst with strong and weak acid sites exhibited bi-functional role. The lower amount of strong acid sites and larger amount of weak acid sites in the synthesized catalyst were conducive to the catalytic performance for MTO under relatively lower reaction temperature. Consequently, the synthesized SSZ-13 showed a better conversion rate and lifetime than that of purchased one. The methanol conversion rate using synthesized catalyst was maintained over 95% within 120 min, and its lifetime was achieved to 172 min. The appropriate acidity and well-developed pore structure of synthesized SSZ-13 could slow down the carbon deposition rate and significantly increase the lifetime of the catalyst. Moreover, the initial selectivity of light olefin could maintain above 50% within 160 min. Eventually, the desirable features of synthesized SSZ-13 catalyst were thought be with good potential for industrial application.

Declarations

Availability of data and materials

All data generated or analyzed during this study are included in this published article [and its supplementary information files].

Competing interests

The authors certify that they have no affiliations with or involvement in any organization or entity with any financial interest or non-financial interest such as personal or professional relationships in the subject matter or materials discussed in this manuscript.

Authors' contributions

Xiongchao Lin: Writing, funding.

Sasha Yang: Writing, experimental

Xiaojia Li: experimental, analysis

Caihong Wang: analysis

Yonggang Wang: analysis

Acknowledgments

This work was supported by the National Natural Science Foundation of China [grant numbers 21978319, 22008253, 21406261]; National Key Research and Development Program [Grant number 2016YFB0600303031] and Yueqi Outstanding Scholar Project (Project Number 2020JCB02).

References

1. Borodina E., Meirer F., Lezcano-González I., Mokhtar M., Asiri A. M., Al-Thabaiti S. A., Weckhuysen B. M., (2015) Influence of the Reaction Temperature on the Nature of the Active and Deactivating Species during Methanol to Olefins Conversion over H-SSZ-13. Acs Catal. 5: 992-1003. https://doi.org/10.1021/acscatal.7b01497.
2. Cheng K., Gu B., Liu X., Kang J., Zhang Q., Wang Y., (2016) Direct and highly selective conversion of synthesis gas into lower olefins: design of a bifunctional catalyst combining methanol synthesis and carbon–carbon coupling. Angew Chem. 128:4803-4806. https://doi.org/10.1002/anie.201601208.
3. Deimund M. A., Harrison L., Lunn J. D., Liu Y., Malek A., Shayib R., Davis M. E., (2016) Effect of heteroatom concentration in SSZ-13 on the methanol-to-olefins reaction. Acs Catal. 6:542-550. https://doi.org/10.1021/acscatal.5b01450.
4. Ferri P., Li C., Millán R., Martínez-Triguero J., Moliner M., Boronat M., Corma A., (2020) Impact of Zeolite Framework Composition and Flexibility on Methanol-To-Olefins Selectivity: Confinement or Diffusion? Angew Chem Intel Ed. 132:1-9. https://doi.org/10.1002/anie.202007609.
5. Han L., Jiang X. G., Lu T. L., Wang B. S., Xu J., Zhan Y. Z., Zhao C., (2017) Preparation of composite zeolites in polymer hydrogels and their catalytic performances in the methanol-to-olefin reaction. Fuel Process Technol. 165: 87-93. https://doi.org/10.1016/j.fuproc.2017.05.018.
6. Janssen A. H., Schmidt I., Jacobsen C. J. H., Koster A.J., Jong K. P. D., (2003) Exploratory study of mesopore templating with carbon during zeolite synthesis. Micropor Mesopor Mat. 65: 59-75. https://doi.org/10.1016/j.micromeso.2003.07.003
7. Jun J. W., Khan N. A., Seo P. W., Kim C. U., Kim H. J., Jhung S. H., (2016) Conversion of Y into SSZ-13 zeolites and ethylene-to-propylene reactions over the obtained SSZ-13 zeolites. Chem Eng J. 303: 667-674. https://doi.org/10.1016/j.cej.2016.06.043.
8. Liu B., Zhou R., Bu N., Wang Q., Zhong S., Wang B., Hidetoshi K., (2017) Room-temperature ionic liquids modified zeolite SSZ-13 membranes for CO_2/CH_4 separation. J Membr Sci. 524: 12-19. https://doi.org/10.1016/j.memsci.2016.11.004.
9. Li D., Xing B., Wang B., Li R., (2020) Activity and selectivity of methanol-to-olefin conversion over Zr-modified H-SAPO-34/H-ZSM-5 zeolites-A theoretical study. Fuel Process Technol. 199: 106302. https://doi.org/10.1016/j.fuproc.2019.106302.
10. Li X., Shen W., Zheng A., (2019) The influence of acid strength and pore size effect on propene elimination reaction over zeolites: A theoretical study. Micropor Mesopor Mat. 278: 121-129. https://doi.org/10.1016/j.micromeso.2018.11.026.

11. Li Z., Navarro M. T., Martínez-Triguero J., (2016) Synthesis of nano-SSZ-13 and its application in the reaction of methanol to olefins. Catal Sci Technol. 6: 5856-5863. DOI https://doi.org/10.1039/C6CY00433D.
12. Sommer L., Mores D., Svelle S., Stöcker M., Weckhuysen B. M., Olsbye U., (2010) Mesopore formation in zeolite H-SSZ-13 by desilication with NaOH. Micropor Mesopor Mat. 132: 384-394. https://doi.org/10.1016/j.micromeso.2010.03.017.
13. Tang T., Yin C., Wang L., (2008) Good sulfur tolerance of a mesoporous Beta zeolite-supported palladium catalyst in the deep hydrogenation of aromatics. J Catal. 257:125-133. https://doi.org/10.1016/j.jcat.2008.04.013.
14. Tian P., Wei Y., Ye M., Liu Z., (2015) Methanol to olefins (MTO): from fundamentals to commercialization. Acs Catal. 5: 1922-1938. https://doi.org/10.1021/acscatal.5b00007.
15. Wang J., Peng Z., Chen Y., Bao W., Chang L., Feng G., (2015) In-situ hydrothermal synthesis of Cu-SSZ-13/cordierite for the catalytic removal of NO_x from diesel vehicles by NH_3. Chem Eng J. 263:9-19. https://doi.org/10.1016/j.cej.2014.10.086.
16. Wardani M., Kadja G., Fajar A., Makertihartha I., Gunawan M., Suendo V., Mukti R., (2019) Highly crystalline mesoporous SSZ-13 zeolite obtained via controlled post-synthetic treatment. RSC Adv. 9: 77-86. DOI https://doi.org/10.1039/C8RA08979E.
17. Wu L., Hensen E. J., (2014) Comparison of mesoporous SSZ-13 and SAPO-34 zeolite catalysts for the methanol-to-olefins reaction. Catal Today. 235:160-168. https://doi.org/10.1016/j.cattod.2014.02.057.
18. Xiao F. S., Wang L., Yin C., (2006) Catalytic properties of hierarchical mesoporous zeolites templated with a mixture of small organic ammonium salts and mesoscale cationic polymers. Angew Chem Int Ed. 45:3090-3093. https://doi.org/10.1002/ange.200600241.
19. Xu R., Zhang R., Liu N., Chen B., Zhang S., (2015) Template Design and Economical Strategy for the Synthesis of SSZ-13 (CHA-Type) Zeolite as an Excellent Catalyst for the Selective Catalytic Reduction of NO_x by Ammonia. Chem Cat Chem. 7:3842-3847. https://doi.org/10.1002/cctc.201500771.
20. Zhang X. Y., Dou T. T., Yao W., Yang J. Y, Wang X., Guo Y. Y., Shen Q., Zhang X., Zhang S. Q., (2019) Green synthesis of Cu-SSZ-13 zeolite by seed-assisted route for effective reduction of nitric oxide. J Clean Prod. 236:117667. https://doi.org/10.1016/j.jclepro.2019.117667.
21. Zeng L., Yu Z., Sun Z., Han Y., Xu Y., Wu J., Wang Z., (2020) Fast synthesis of SSZ-13 zeolite by steam-assisted crystallization method. Micropor Mesopor Mat. 293:109789. https://doi.org/10.1016/j.micromeso.2019.109789.
22. Zhou Y., Qi L., Wei Y., Yuan C., Zhang M., Liu Z., (2016) Methanol-to-olefin induction reaction over SAPO-34. Chinese J Catal. 37:1496-1501. https://doi.org/10.1016/S1872-2067(15)61110-X.
23. Zhu X., Hofmann J. P., Mezari B., (2016) Trimodal Porous Hierarchical SSZ-13 Zeolite with Improved Catalytic Performance in the Methanol-to-Olefins Reaction. ACS Catal. 6:2163-2177. https://doi.org/10.1021/acscatal.5b02480.

24. Zhu X., Rohling R., Filonenko G., Mezari B., Hofmann J. P., Asahina S., Hensen E. J., (2014) Synthesis of hierarchical zeolites using an inexpensive mono-quaternary ammonium surfactant as mesoporogen. Chem Commun. 50: 14658-14661. https://doi.org/10.1039/C4CC06267A.

Figures

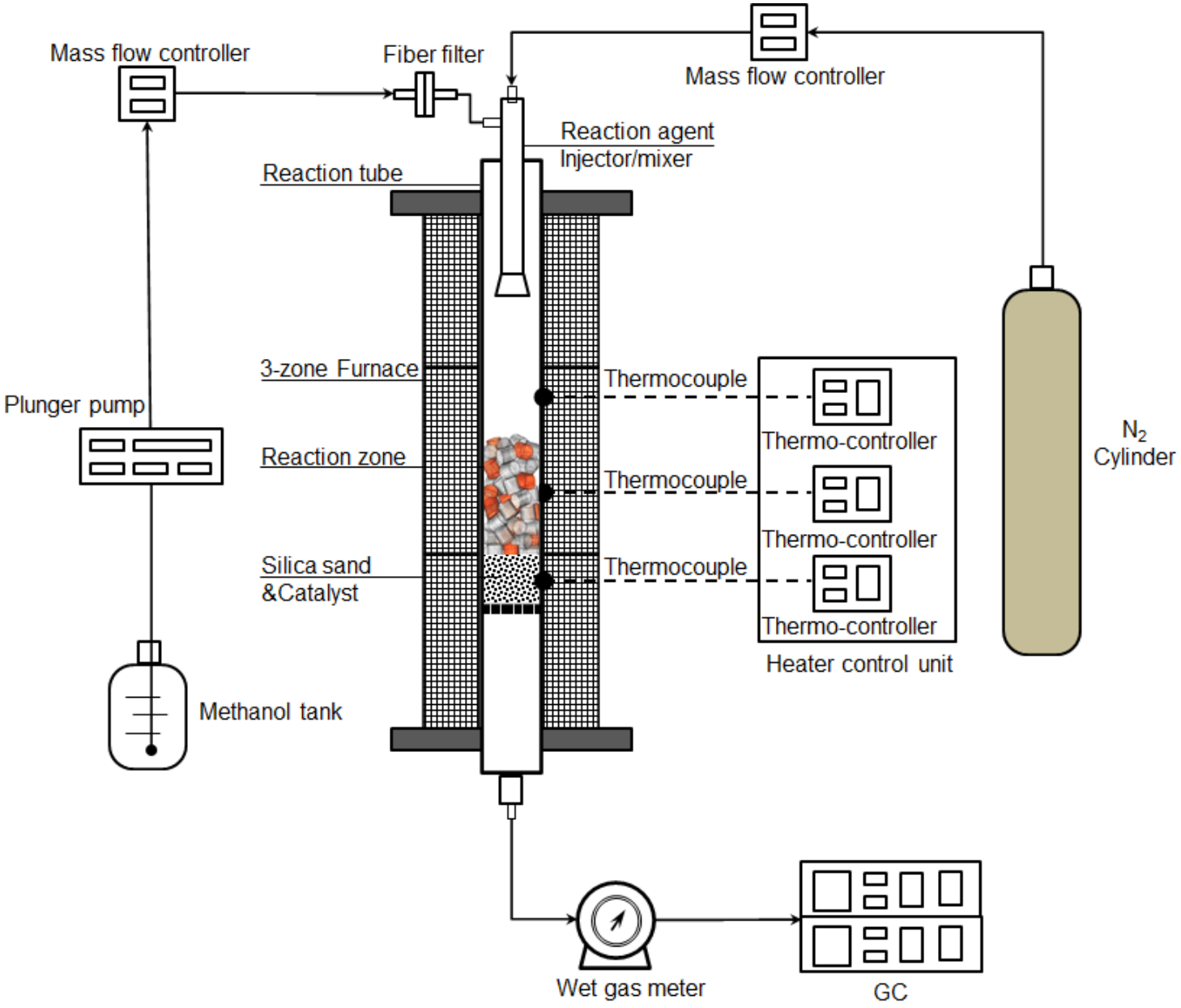

Figure 1

Schematic of the fixed-bed reactor

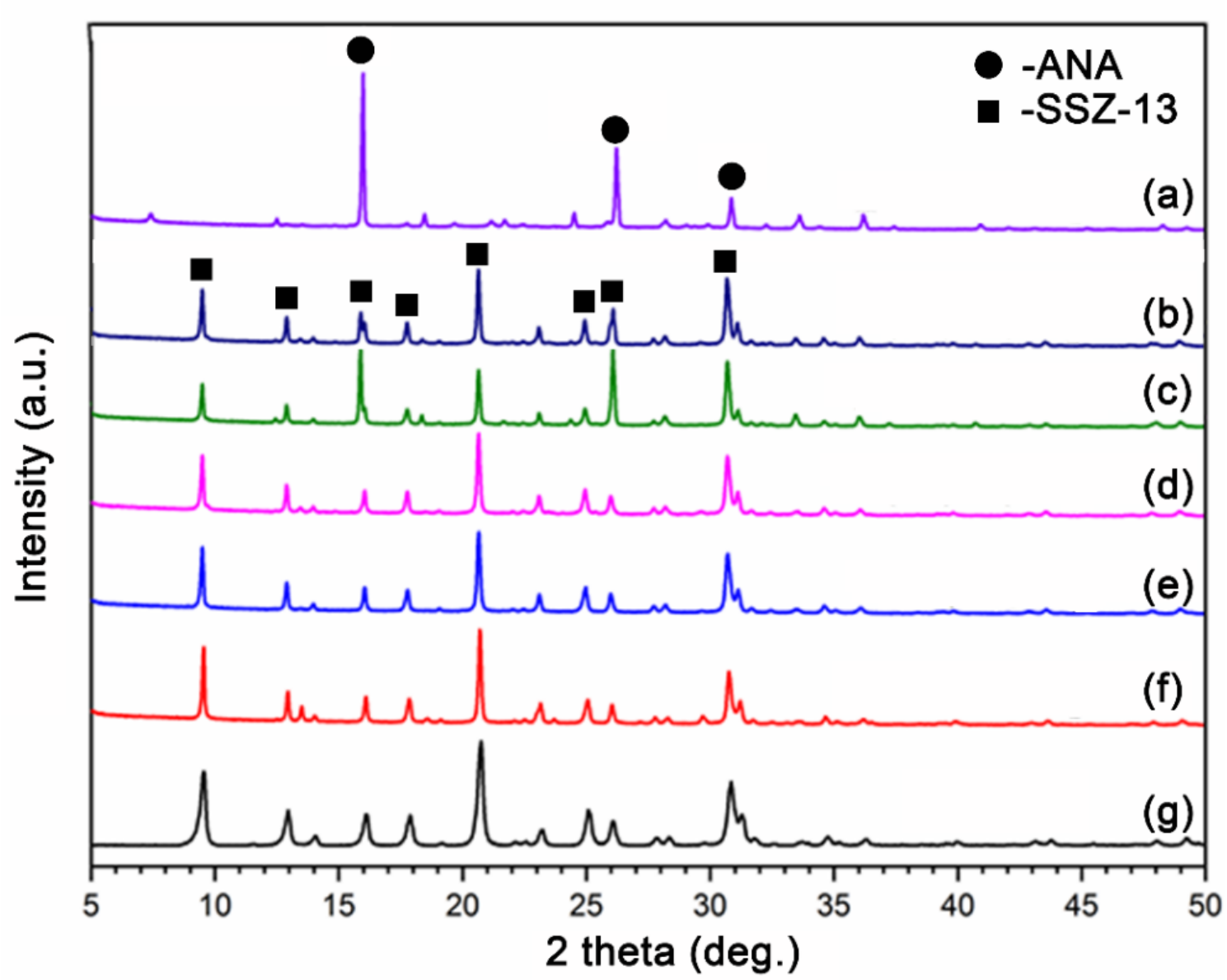

Figure 2

XRD of SSZ-13 zeolite prepared with different m(CC)/m(SiO2), (a) 0, (b) 0.07, (c) 0.11, (d) 0.14, (e) 0.21, (f) 0.32, and (g) purchased SSZ-13.

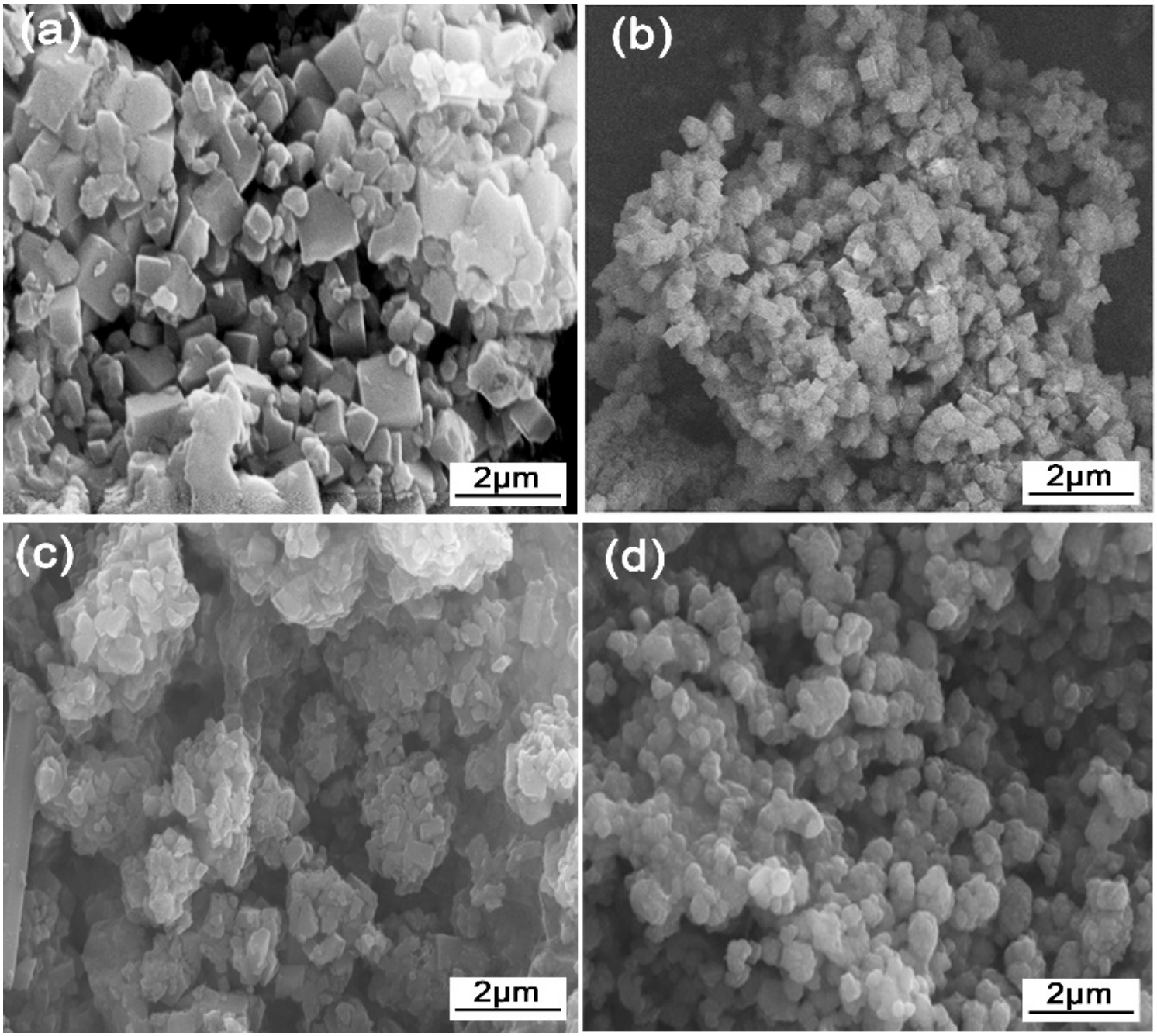

Figure 3

SEM images of SSZ-13 zeolite prepared at different ratios of m(CC)/m(SiO2) (a) 0.07, (b) 0.14, (c) 0.32, and (d) purchased SSZ-13.

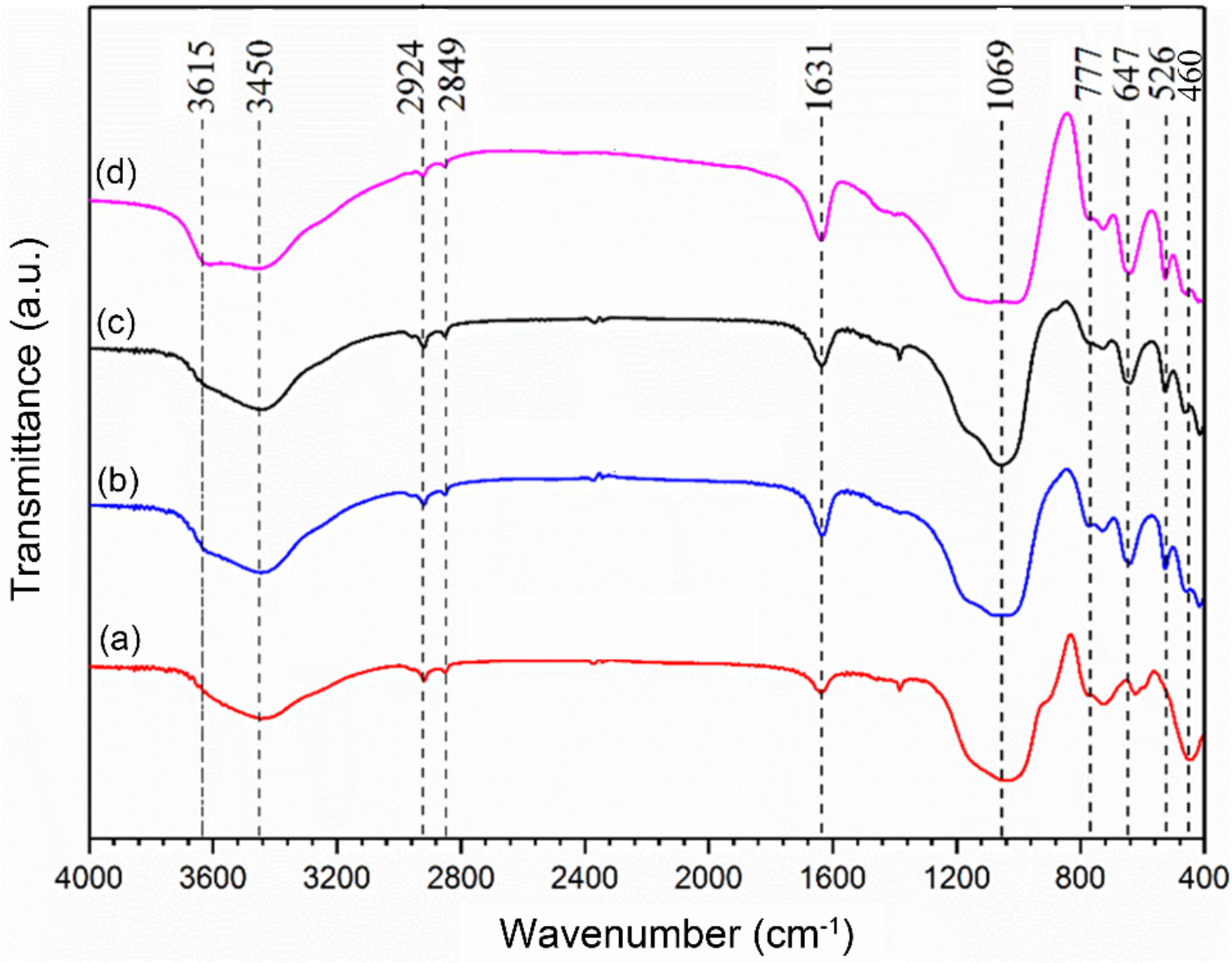

Figure 4

FTIR spectra of synthesized zeolite with different m(CC)/m(SiO2) (a) 0, (b) 0.07, (c) 0.14, and (d) 0.32

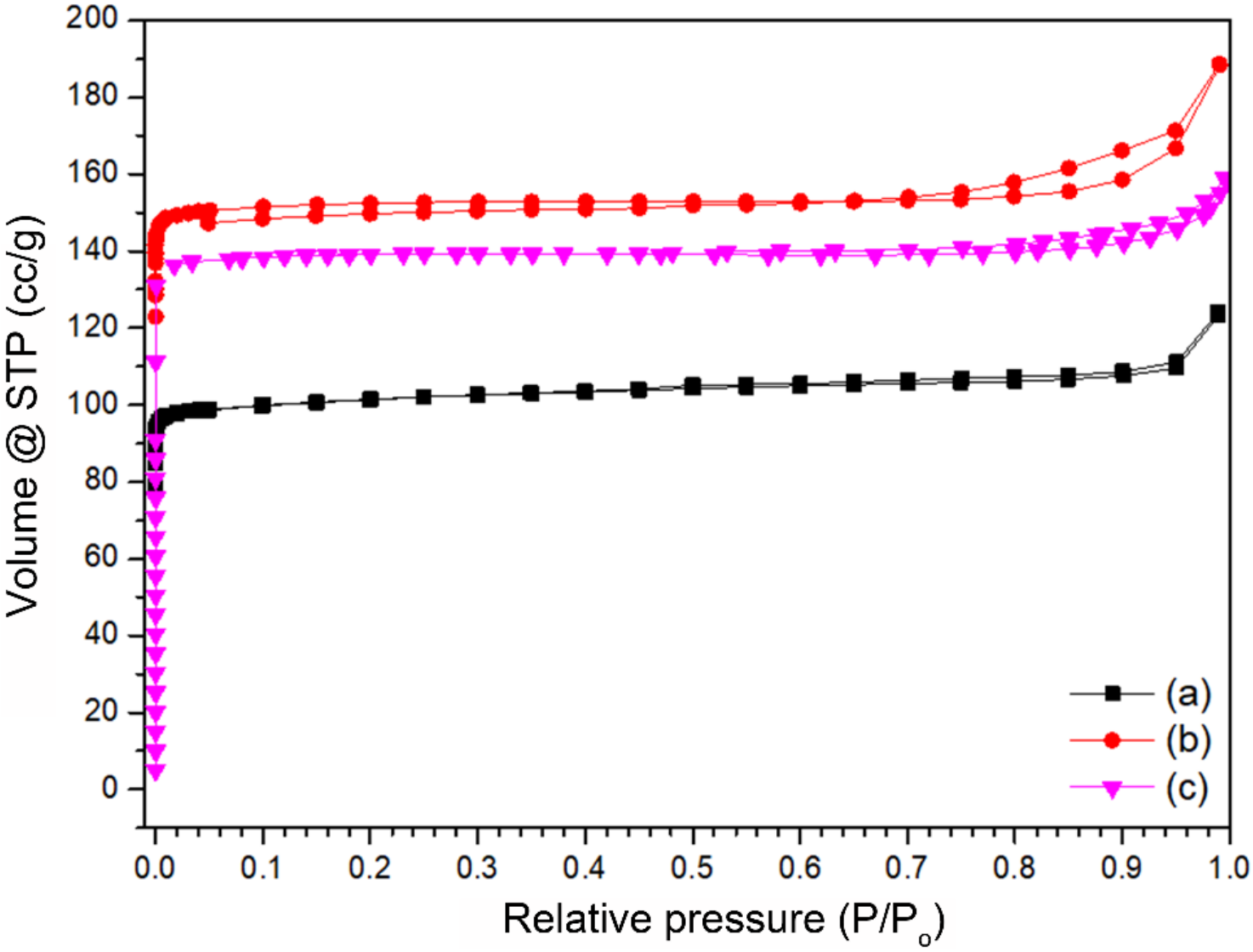

Figure 5

Nitrogen adsorption-desorption isotherms of zeolite prepared with different m(CC)/m(SiO2), (a) 0.07, (b) 0.14, and (c) 0.32.

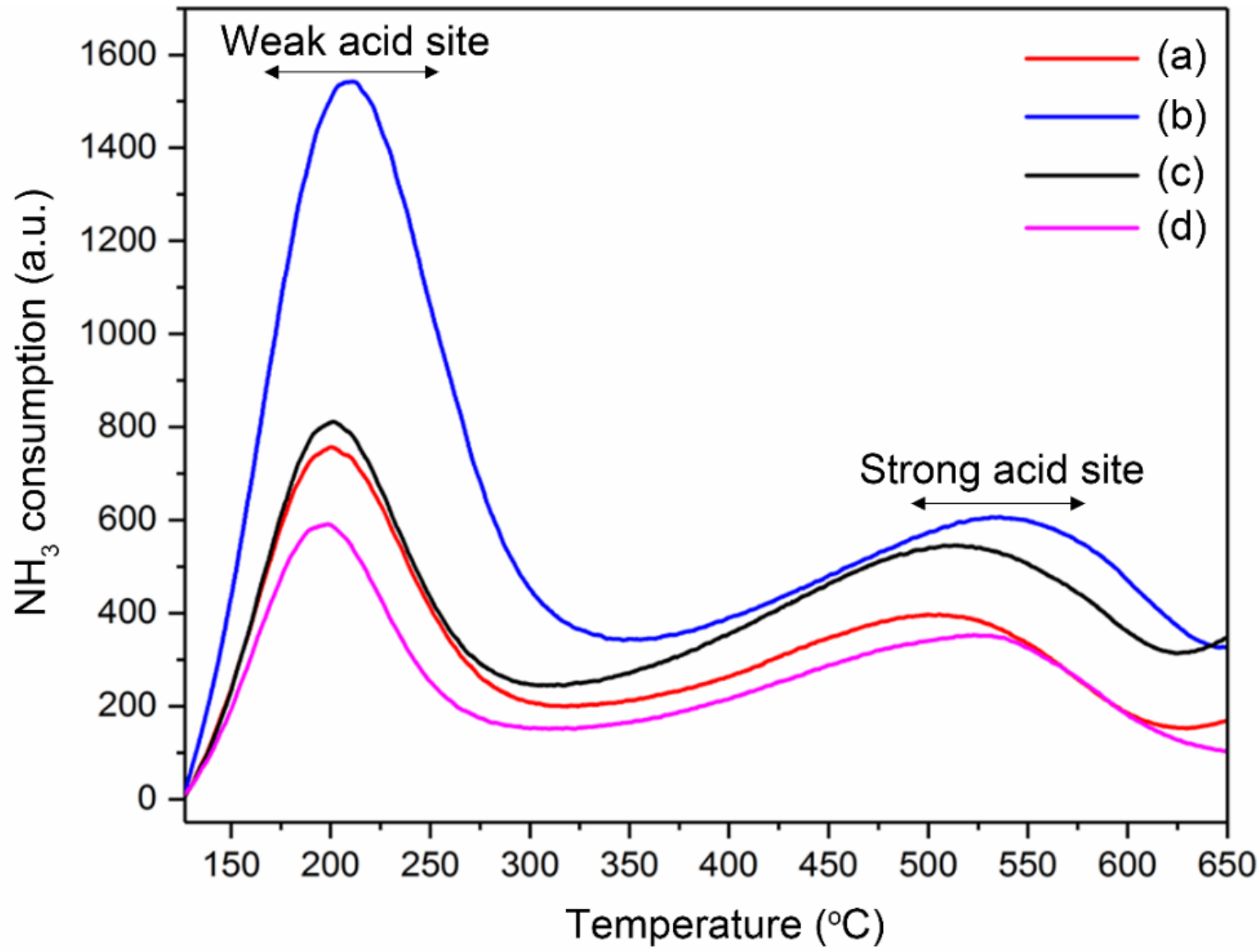

Figure 6

NH3-TPD of samples with different m(CC)/m(SiO2) (a) 0.07, (b) 0.14, (c) 0.32, and purchased SSZ-13.

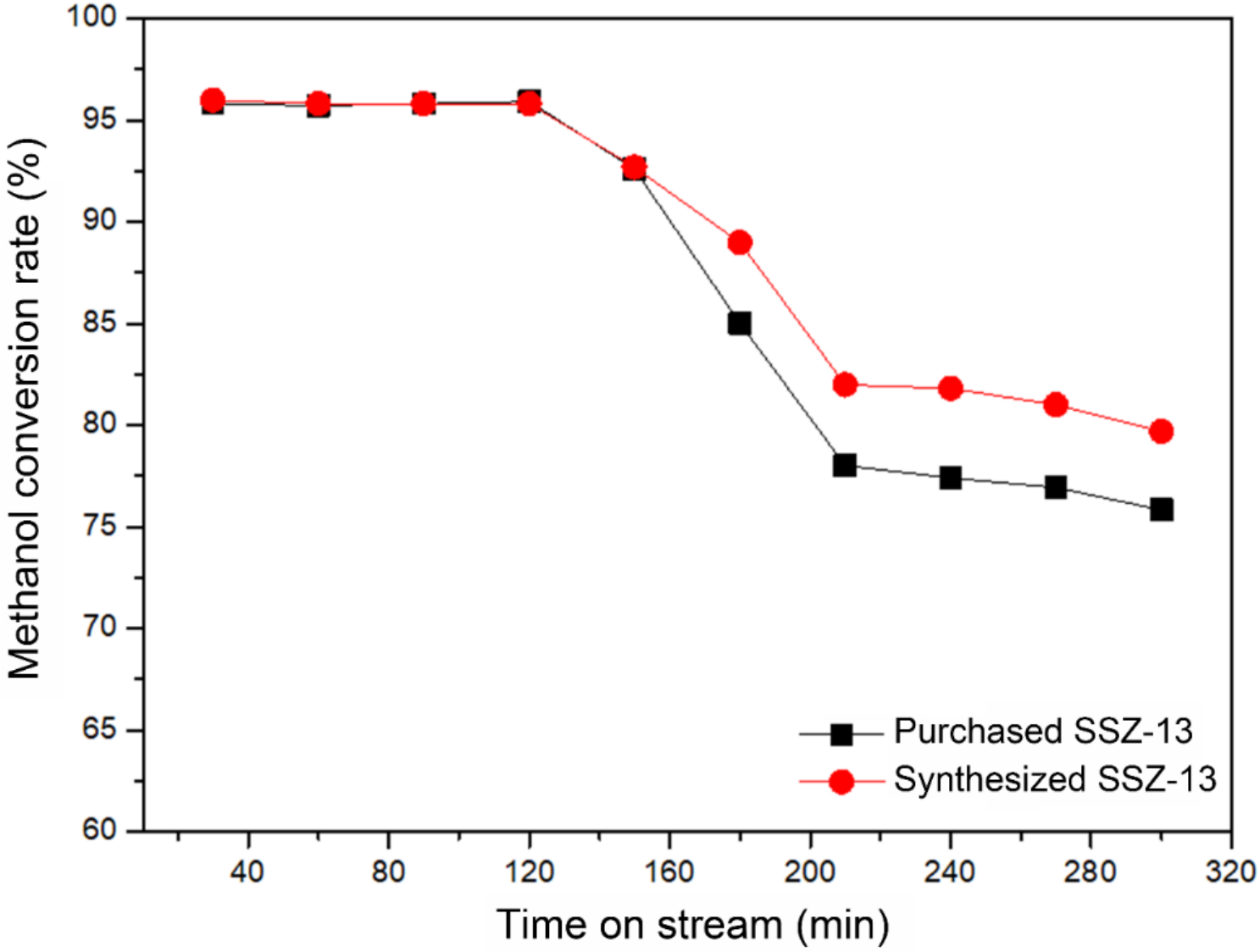

Figure 7

The methanol conversion rate of purchased and synthesized SSZ-13 catalysts.

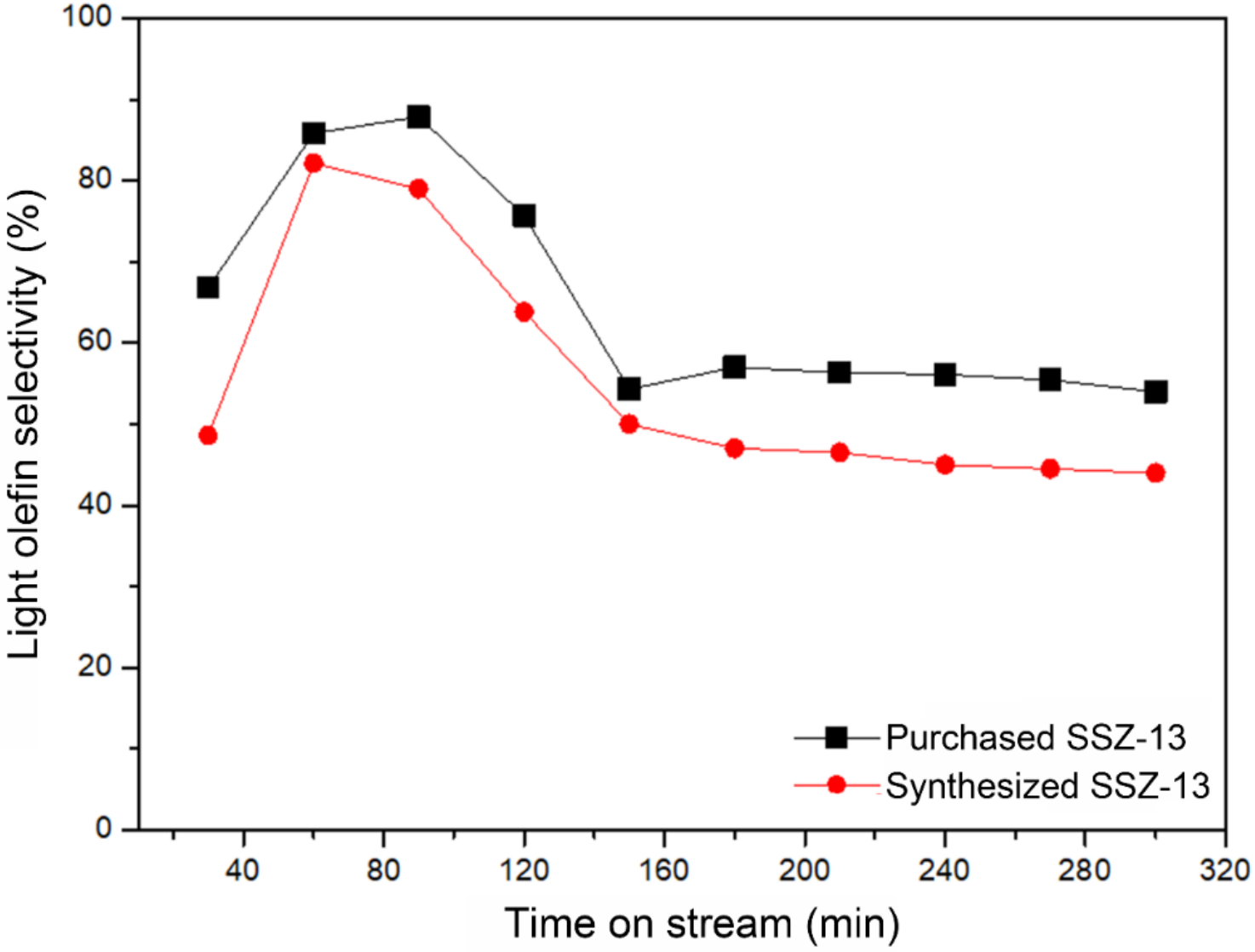

Figure 8

The low olefin selectivity of purchased and synthesized SSZ-13 catalysts.

Supplementary Files

This is a list of supplementary files associated with this preprint. Click to download.

- supportinginformation.docx